2264 J. Med. Chem. 2010, 53, 2264–2276
DOI: 10.1021/jm901852f

Journal of Medicinal Chemistry Article

Synthesis and Biological Evaluation of Botulinum Neurotoxin A Protease Inhibitors

Bing Li,*,† Ramdas Pai,† Steven C. Cardinale,† Michelle M. Butler,† Norton P. Peet,† Donald T. Moir,† Sina Bavari,‡ and Terry L. Bowlin†

†Microbiotix Inc., One Innovation Drive, Worcester, Massachusetts 01605, and ‡United States Army Medical Research Institute of Infectious Diseases, Fort Detrick, Frederick, Maryland 21702

Received December 15, 2009

NSC 240898 was previously identified as a botulinum neurotoxin A light chain (BoNT/A LC) endopeptidase inhibitor by screening the National Cancer Institute Open Repository diversity set. Two types of analogues have been synthesized and shown to inhibit BoNT/A LC in a FRET-based enzyme assay, with confirmation in an HPLC-based assay. These two series of compounds have also been evaluated for inhibition of anthrax lethal factor (LF), an unrelated metalloprotease, to examine enzyme specificity of the BoNT/A LC inhibition. The most potent inhibitor against BoNT/A LC in these two series is compound **12** (IC_{50} = 2.5 μM, FRET assay), which is 4.4-fold more potent than the lead structure and 11.2-fold more selective for BoNT/A LC versus the anthrax LF metalloproteinase. Structure−activity relationship studies have revealed structural features important to potency and enzyme specificity.

Introduction

Botulinum neurotoxins (BoNTs[a]) secreted by strains of the anaerobic spore-forming bacterial species *Clostridium botulinum* are the most potent neurotoxins known and are categorized as category A (highest priority) bioterrorist agents by the Centers for Disease Control and Prevention (CDC).[1,2] BoNTs represent a significant bioterrorist threat because they can be used as biological warfare agents in a highly toxic aerosol form or added to food.[2−5] Among the seven BoNT serotypes (A−G), BoNT serotype A (BoNT/A) is the deadliest and the most threatening with a lethal dose of 1.0 ng/kg in humans and is accompanied by a prolonged half-life.[2,6] Structurally, BoNTs are composed of a 100 kDa heavy chain (HC) and a 50 kDa light chain (LC) linked by a disulfide bond. The LC is a zinc-dependent endopeptidase that catalyzes the cleavage of a component of the SNARE proteins (soluble *N*-ethylmaleimide-sensitive factor attachment protein receptor). BoNT serotypes A and E cleave SNAP-25 (synaptosomal-associated protein, 25 kDa); serotypes B, D, F, and G cleave VAMP (vesicle-associated membrane protein, also referred to as synaptobrevin); and serotype C cleaves both SNAP-25 and syntaxin 1.[7−9] BoNT-mediated cleavage of the SNARE proteins interrupts the function of motor nerves via the inhibition of acetylcholine release and produces flaccid paralysis and potential death of the infected patients.[6] Even though BoNT toxoid vaccine showed efficacy in the prevention of botulism poisoning, it is only available to consenting military personnel and research workers who are actively handling the toxins. Moreover, the vaccine cannot counter these toxins after they penetrate neurons. Currently, the only therapies for BoNT intoxication include experimental preventative antibodies and long-term supportive care (e.g., mechanical ventilation).[10−12] However, the antibodies can cause severe side effects, such as serum sickness and anaphylaxis, and mechanical ventilation is not practical when large populations are threatened by the toxins. New, small molecule therapeutic BoNT inhibitors, especially those that are active postexposure (e.g., rescue therapeutics), are vital to the biodefense arsenal.

BoNT/A light chain (BoNT/A LC) has been widely studied as a drug target for the discovery and development of inhibitors of botulinum neurotoxins. Schmidt and Rich et al.[13] have developed peptide and peptidomimetic inhibitors of BoNT/A LC around the substrate SNAP-25 cleavage site with submicromolar to low micromolar K_i values. A series of 4-aminoquinolines have been identified, which prevent BoNT/A-induced SNAP-25 cleavage.[14] Boldt et al.[15] have reported that a D-cysteine derivative was a BoNT/A LC inhibitor that also demonstrated cellular activity. Cinnamic acid hydroxamate **1** (Figure 1) was shown to inhibit BoNT/A LC with a K_i value of 0.3 μM and an IC_{50} value of 0.41 μM.[16] Moe et al.[17] described a series of mercaptoacetamide inhibitors (example 2, Figure 1) active against botulinum neurotoxin A with low micromolar potency. Recently, a quinolinol derivative **3** (Figure 1) has been reported as a BoNT/A LC inhibitor with an IC_{50} value of 0.5 μM in a tissue-based ex vivo assay,[18] and this type of compound inhibits BoNT/A LC in a noncompetitive manner.[19] A tetrasubstituted pyrrole inhibitor (compound **4**, Figure 1), created by synthesis-based computer-aided molecular design, displayed BoNT/A inhibition with a K_i value of 0.76 ± 0.17 μM and an IC_{50} value of < 1 μM.[20] Burnett et al.[21] have designed and synthesized a hybrid inhibitor using a three-zone pharmacophore model

*To whom correspondence should be addressed. Phone: +1-508-757-2800. Fax: +1-508-757-1999. E-mail: bli@microbiotix.com.

[a]Abbreviations: BoNTs, botulinum neurotoxins; BoNT/A, botulinum neurotoxin serotype A; BoNT/B, botulinum neurotoxin serotype B; BoNT/A HC, botulinum neurotoxin serotype A heavy chain; BoNT/A LC, botulinum neurotoxin serotype A light chain; LF, lethal factor; FRET, fluorescence resonance energy transfer; HPLC, high performance liquid chromatography; MMPs, matrix metalloproteases.

 Published on Web 02/15/2010

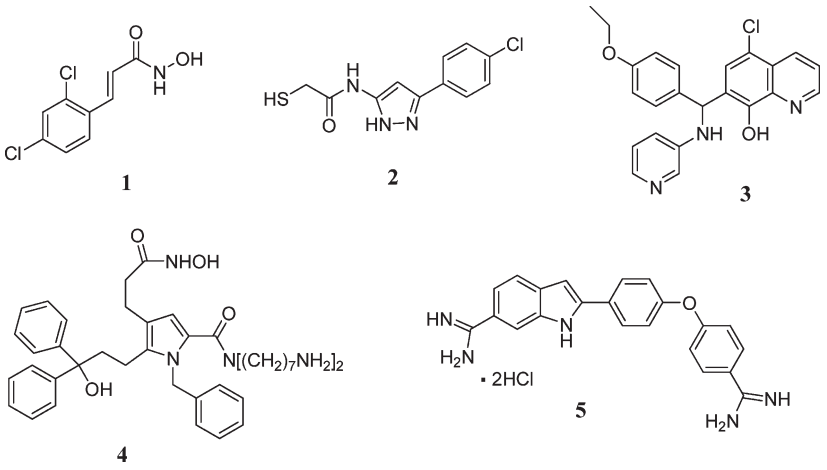

Figure 1. Small-molecule inhibitors of BoNT/A LC.

to link an indole bis-amidine structure[22] with a 4-amino-7-chloroquinoline,[23] which exhibits a K_i value of 0.6 μM vs BoNT/A LC. A series of benzylidene cyclopentenedione-based inhibitors were shown to inactivate BoNT/A LC through covalent modification of the enzyme in a biochemical assay.[24]

Indole bis-amidine **5** (NSC 240898, Figure 1) is a potent BoNT/A LC endopeptidase inhibitor identified from screening a collection of the National Cancer Institute's Open Repository diversity set, using a high throughput fluorescence resonance energy transfer (FRET) assay combined with a molecular modeling approach. The activity of this lead compound has been verified using an HPLC-based confirmatory assay.[22] Compound **5** exhibited 75% inhibition of the BoNT/A LC endopeptidase at 20 μM, and no cytotoxicity was detected at concentrations as high as 40 μM. It was also found to be neuron-permeable. These findings show that **5** is a promising lead compound for further optimization. During our ongoing research, Wang et al.[25] reported the synthesis and preliminary structure−activity relationship studies based on compound **5**; however, no significant improvement in potency was reported by these authors. Here, we report the syntheses of two types of analogues of compound **5** and their inhibitory activities against BoNT/A LC and anthrax LF metalloprotease in FRET-based enzyme assays.

Results and Discussion

Chemistry. Compound **5** is a bis-amidine comprising an indole core structure with a phenoxyphenyl moiety at the 2-position. To improve the in vitro activity against BoNT/A LC, we designed the two types of analogues shown in Figure 2. Type I inhibitors consist of an indole, benzothiophene, or benzimidazole core structure and bear a 4-(phenoxy)aryl group at the 2-position. The heteroatom on the heterocyclic core was proposed either to interact directly with the active site Zn or to hydrogen-bond with catalytic water molecules.[26,27] Type II inhibitors also have an indole or benzothiophene core structure with an aryl group at the 2-position.

Type I analogues **10**−**15** were prepared from dinitrile **9**, which was produced via a Cadogan−Sundberg indole synthesis (Scheme 1). 4-Hydroxybenzaldehyde (**6**) was treated with 4-fluorobenzonitrile to give aldehyde **7**, which was then condensed with 4-methyl-3-nitrobenzonitrile to give **8**. Stilbene **8** underwent a Cadogan−Sundberg reaction to afford

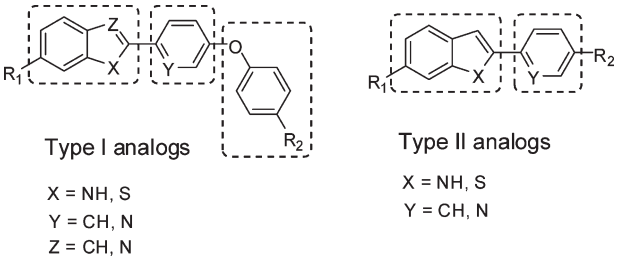

Figure 2. Two types of analogues of BoNT/A LC inhibitor **5**.

dinitrile **9** in 55% yield. Treatment of dintrile **9** with 4:1 (v/v) TFA/H_2SO_4 gave diamide **10**. Interestingly, a monoamidine product **11** was isolated exclusively when dinitrile **9** was treated with the amidination agent $LiN(TMS)_2$.

The imidate intermediate obtained from the Pinner reaction with dinitrile **9** was treated with *N*,*N*-dimethylethylenediamine to produce the *N*,*N*-dimethylethylene-substituted bis-amidine compound **12**, which was isolated by HPLC purification. The dinitrile **9** was also treated with diamines in the presence of P_2S_5 to give bis-amidines **13**−**15**.

Dinitriles **23a**−**c** were prepared by using a Suzuki coupling protocol with boronic acids **20a**,**b** and phenoxyarylbromides **19a**−**c**, which were obtained by condensation of compounds **17a**,**b** with aryl fluorides **18a**,**b**. The coupling products were further elaborated to type I analogues **24a**−**c** and **25a**,**b** (Scheme 2). Compounds **24a**,**b** and **25a**,**b** were bis-amidine compounds, and **24c** was isolated as a monoimidazoline compound after HPLC purification.

Type I analogues **29** and **32** contain only one imidazoline group on either the indole ring or the phenyl ring. Syntheses of **29** and **32** are shown in Schemes 3 and 4, respectively. Nitrile intermediates **28** and **31** were prepared by Suzuki coupling of corresponding boronic acids **20a** and **30** with the 4-phenoxyphenyl bromides **27** and **19a**, respectively, followed by treatment with ethylenediamine in the presence of P_2S_5 to give imidazolines **29** and **32**.

Syntheses of type I analogues **35a**,**b** with a benzimidazole core structure are shown in Scheme 5. Oxidative condensation of 4-cyanophenylenediamine (**33**) with aldehyde **7** provided dinitrile **34**, which was then converted to bis-imidazoline **35a** and bis-tetrahydropyrimidine **35b** using a P_2S_5-mediated cyclization reaction.

Syntheses of type II inhibitors **40a**−**c**, **43a**−**c**, and **44a**,**b** with indole core structures are shown in Schemes 6 and 7.

Scheme 1. Syntheses of Type I Analogues **10**−**15**[a]

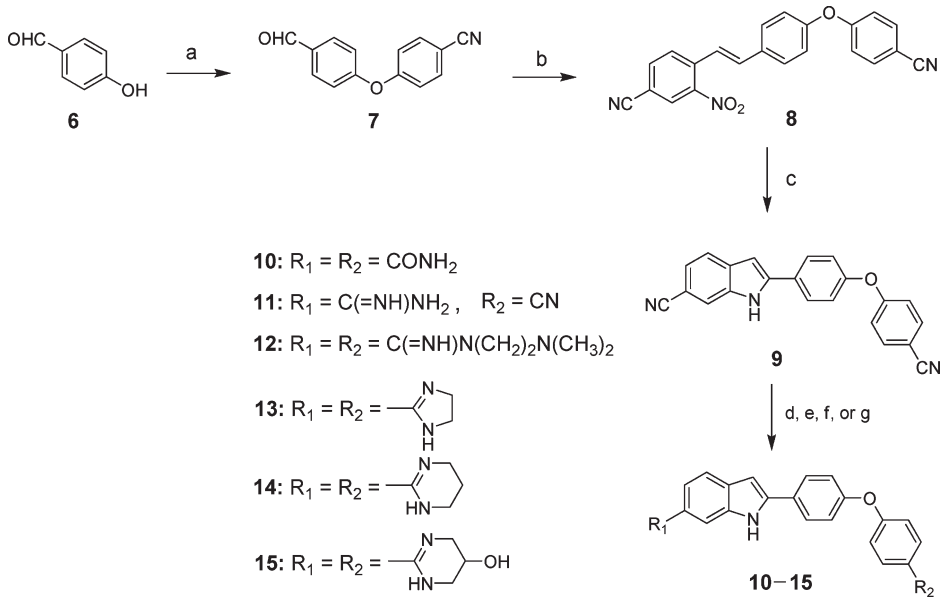

[a] Reagents and conditions: (a) 4-fluorobenzonitrile, K_2CO_3, DMF, 150−160 °C, 87%; (b) 4-methyl-3-nitrobenzonitrile, piperidine, 150 °C, 67%; (c) $P(OEt)_3$, reflux, 55%; (d) TFA/H_2SO_4 (4:1), room temp, 83% for **10**; (e) $LiN(TMS)_2$, THF, 83% for **11**; (f) (i) HCl (g), dry EtOH; (ii) 10 equiv of *N*,*N*-dimethylethylenediamine, dry EtOH, 25% for **12**; or 10 equiv of 1,3-diaminopropan-2-ol, dry EtOH, 84% for **15**; (f) P_2S_5, ethylenediamine, 93% for **13**; P_2S_5, 1,3-diaminopropane, 98% for **14**.

Scheme 2. Syntheses of Type I Analogues **24a**−**c** and **25a**,**b**[a]

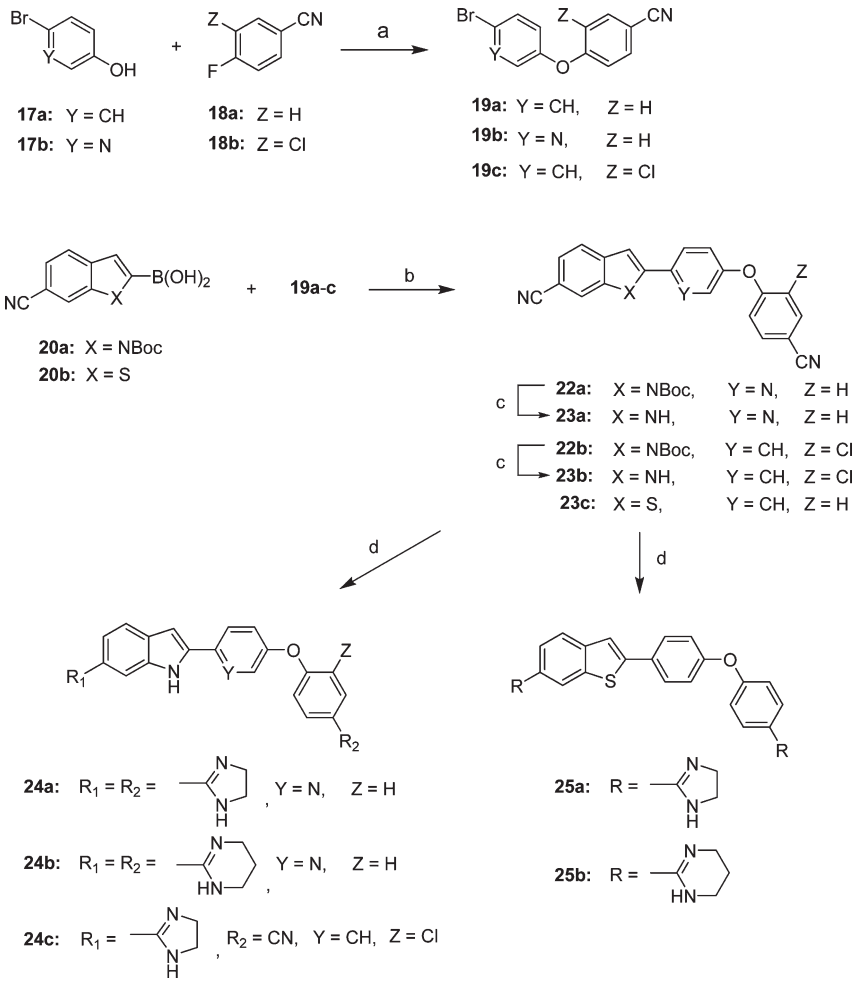

[a] Reagents and conditions: (a) K_2CO_3, DMF, 150 °C; (b) $Pd(PPh_3)_4$, Na_2CO_3, toluene/EtOH/H_2O; (c) TFA/CH_2Cl_2; (d) P_2S_5, ethylenediamine, 120 °C for **24a**, **24c**, and **25a**, or 1,3-diaminopropane, 120 °C for **24b** and **25b**.

Scheme 3. Synthesis of Type I Analogue **29**[a]

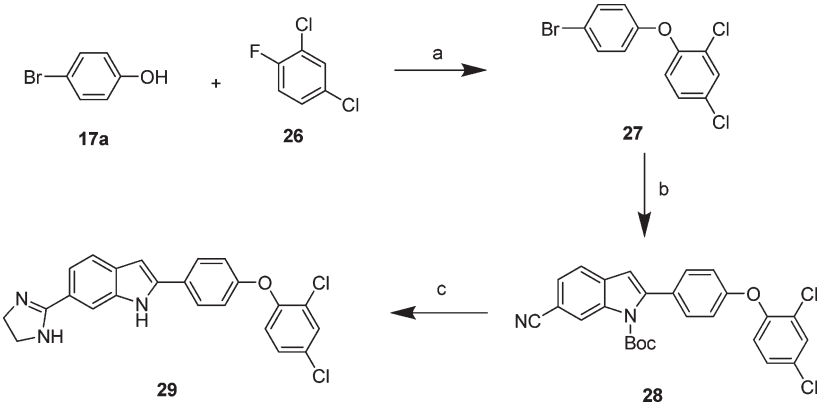

[a] Reagents and conditions: (a) K_2CO_3, DMF, 150−160 °C, 91% yield; (b) **20a**, $Pd(PPh_3)_4$, Na_2CO_3, toluene/EtOH/H_2O, reflux, 49% yield; (c) ethylenediamine, P_2S_5, 120 °C, 64% yield.

Scheme 4. Synthesis of Type I analogue **32**[a]

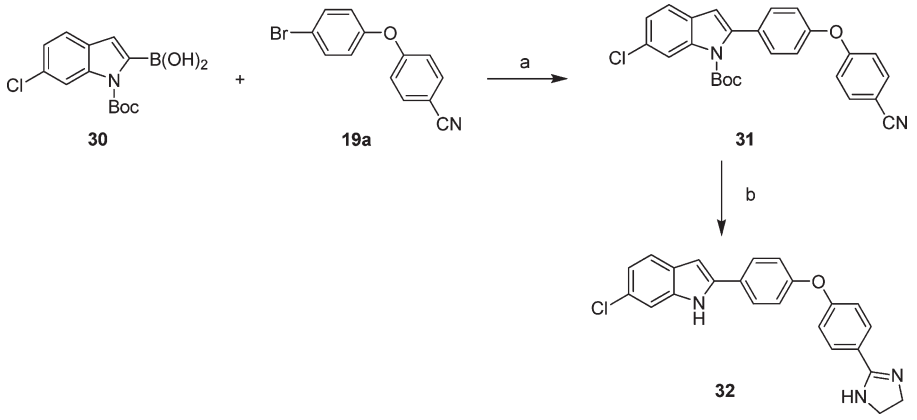

[a] Reagents and conditions: (a), $Pd(PPh_3)_4$, Na_2CO_3, toluene/EtOH/H_2O, reflux, 40% yield; (c) (i) ethylenediamine, P_2S_5, 120 °C, 65% yield.

Scheme 5. Syntheses of Type I Analogues **35a**,**b**[a]

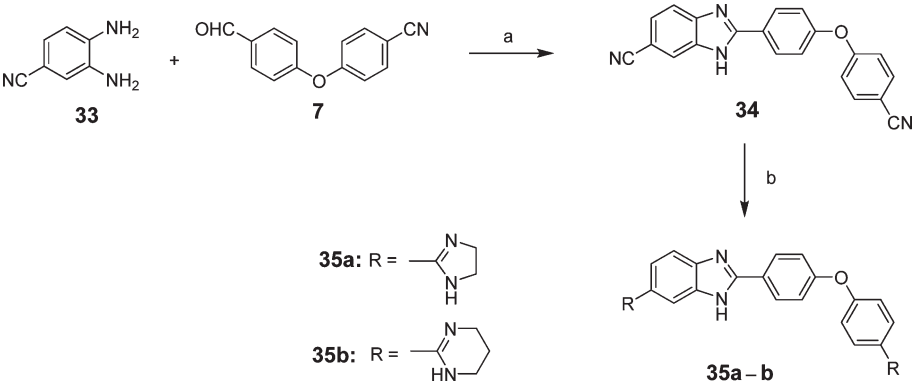

[a] Reagents and conditions: (a) 40% $NaHSO_3$, EtOH, 80 °C, 100% yield; (b) ethylenediamine, P_2S_5, 120 °C for **35a**, 81% yield, or 1,3-diaminopropane, P_2S_5, 120 °C for **35b**, yield 30%.

Condensation of 4-cyano-2-nitrotoluene (**36**) with 4-fluorobenzaldehyde (**37**) gave *o*-nitrostilbene **38**, which underwent a Cadogan−Sundberg indole synthesis to provide nitrile **39** as the major product. Subsequently, amide **40a**, amidine **40b**, and imidazoline **45c** were prepared using the methods previously described (Scheme 6). Suzuki coupling of boronic acid **20a** with aryl bromides **41a**,**b** provided 2-aryl-6-cyanoindoles **42a**,**b**, which were then transformed to type II inhibitors **43a**−**c** and **44a**,**b** using reaction conditions corresponding to those described in Scheme 6 (Scheme 7).

Syntheses of type II inhibitors **46a**,**b**, **49**, and **50** containing a benzothiophene core structure are shown in Schemes 8 and 9. Suzuki coupling of 6-cyanobenzothiophene-2-boronic acid (**20b**) with 4-bromobenzonitrile (**41b**) provided dinitrile **45**, which was then converted to bis-imidazoline **46a** and bis-tetrahydropyrimidine **46b** (Scheme 8). Likewise, Suzuki coupling of boronic acid

Scheme 6. Syntheses of Type II Analogues **40a**−**c**[a]

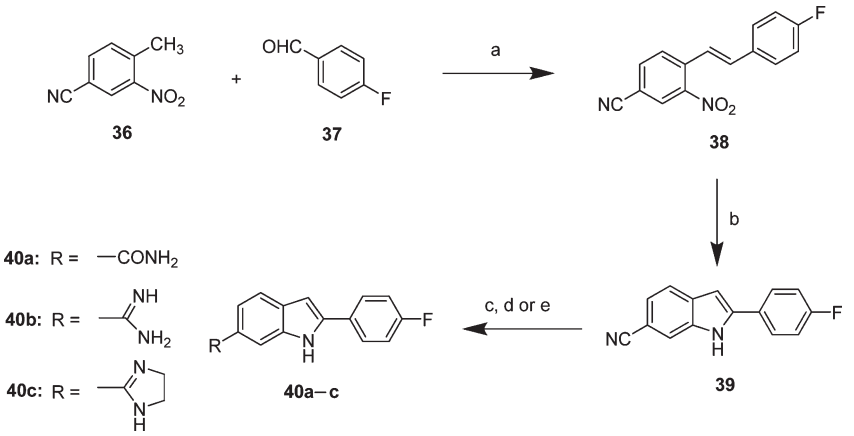

[a] Reagents and conditions: (a) piperidine, 150 °C, 96%; (b) $P(OEt)_3$, reflux, for **39**; (c) TFA/H_2SO_4 (4:1), room temp for **40a**; (d) (i) HCl (gas), dry EtOH; (ii) NH_3(gas), dry EtOH for **40b**, 76% yield; (e) P_2S_5, ethylenediamine, 90% yield for **40c**.

Scheme 7. Synthesis of Type II Inhibitors **43a**−**c** and **44a**,**b**[a]

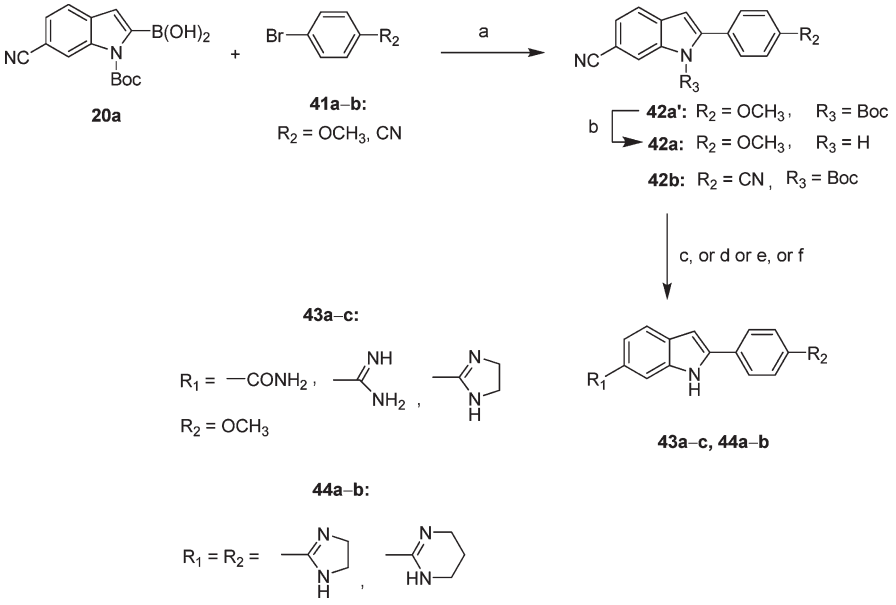

[a] Reagents and conditions: (a) $Pd(PPh_3)_4$, Na_2CO_3, toluene/EtOH/H_2O, 100 °C; (b) TFA/4 N HCl in dioxane (5:1) (c) TFA/H_2SO_4 (4:1), room temp, 40% for **43a**; (d) (i) HCl (g), dry EtOH; (ii) NH_3 (g), dry EtOH, 38% for **43b**; (e) P_2S_5, ethylenediamine, 92% for **43c**; 74% for **44a**; (f) P_2S_5, 1,3-diaminopropane, 68% for **44b**.

Scheme 8. Syntheses of Type II Inhibitors **46**[a]

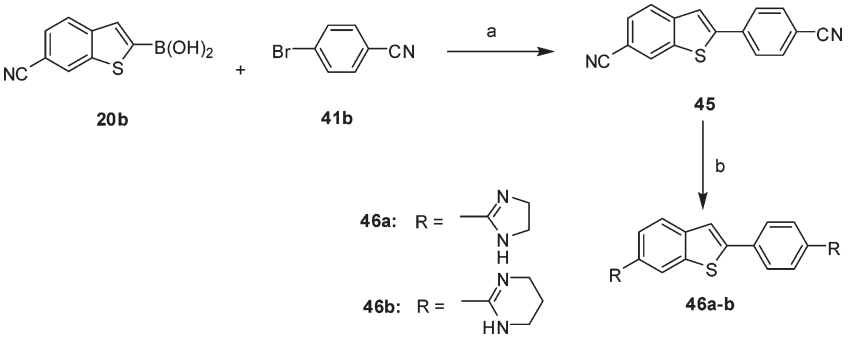

[a] Reagents and conditions: (a) (2-biphenyl)-di-*tert*-butylphosphine, $Pd(OAc)_2$, K_2CO_3, DMF, 100 °C, 90% yield; (b) P_2S_5, ethylenediamine, 87% for **46a**; (c) P_2S_5, 1,3-diaminopropane, 52% for **46b**.

20b with 2-bromo-5-fluoropyridine (**47**) provided nitrile **48**. Treatment of **48** with H_2SO_4/TFA (4:1) and ethylenediamine gave amide **49** and imidazoline **50**, respectively (Scheme 9).

Scheme 9. Syntheses of Type II Inhibitors **49** and **50**[a]

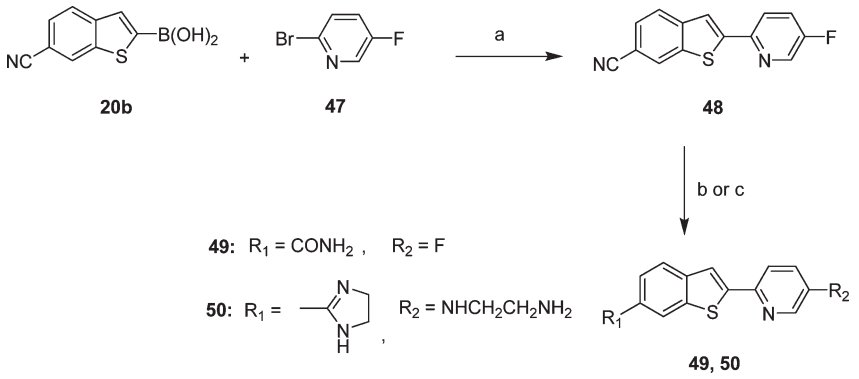

[a] Reagents and conditions: (a) $Pd(PPh_3)_4$, Na_2CO_3, toluene/EtOH/H_2O, 100 °C; (b) TFA/H_2SO_4 (4:1), room temp, 92% for **49**; (c) P_2S_5, ethylenediamine, 30% for **50**.

Biological Evaluation of Type I and Type II Inhibitors. The type I and type II compounds were evaluated in a fluorescence resonance energy transfer (FRET) assay[28] against recombinant BoNT/A LC, and the inhibitory activities are shown in Tables 1 and 2. FRET data for the most potent compounds were confirmed with a secondary HPLC-based assay (data shown in parentheses in Tables 1 and 2). To examine enzyme specificity, compounds were also evaluated in a FRET-based anthrax lethal factor (LF) assay using a previously reported procedure.[28,29] Anthrax LF, a component of the anthrax tripartite exotoxin, is also a zinc-containing metalloprotease, but it has no significant sequence similarity to BoNT/A LC. Compounds exhibiting specificity for BoNT/A LC were further examined in a larger panel of metalloprotease assays.[30]

Generally, neutral groups such as nitriles (**9**, **23a**,**b**, and **39**) or amides (**10**, **40a**, **43a**, and **49**), as substituents on the indole or benzothiophene core structures, diminished the potency against both BoNT/A LC and anthrax LF. Basic groups on the core structures are necessary for botulinum toxin inhibitory activity, and compounds with basic groups on both ends of the scaffold are generally more potent than compounds with one basic group on the scaffold. In the BoNT/A LC assay, for example, bis-amidine **2** exhibited an IC_{50} value of 11 μM vs BoNT/A LC, while monoamidine **11** showed no activity against BoNT/A LC. Monoimidazoline **24c** (BoNT/A LC IC_{50} = 30 μM) is 2.4-fold less potent than bis-imidazoline **13** (IC_{50} = 12.5 μM), suggesting that both basic groups may participate in hydrogen bonding or ionic interactions with the target enzyme.[25] Type I inhibitors with three-ring scaffolds exhibited more potency than type II inhibitors with two-ring scaffolds, when bearing the same substituents. For example, type I inhibitors **13**, **14**, **25a**, and **25b** with three-ring scaffolds bearing imidazoline or tetrahydropyrimidine moieties were more potent against botulinum neurotoxin than their counterpart type II inhibitors with two-ring scaffolds, e.g., compounds **44a**, **44b**, **46a**, and **46b**.

Type I inhibitors with the benzimidazole core structure (**35a** and **35b**) exhibited less potency than type I inhibitors with indole core structures (**13** and **14**), which is consistent with an earlier report.[25] The more basic benzimidazole core structure may be disruptive to the complementary hydrophobic contact of the indole ring with BoNT/A LC. Additional heteroatoms in the indole ring, such as N and S, may interact with the Zn ion in the BoNT/A LC active site or interact with the catalytic site water molecules. However, replacement of a CH unit in the middle ring of the 2-((phenoxy)phenyl)indole scaffold with nitrogen dramatically decreases the inhibitory activity against BoNT/A LC (for example, **13** vs **24a** and **14** vs **24b**). The most potent BoNT/A LC inhibitor in the enzyme-based assay is compound **12**, which exhibited an IC_{50} value of 2.5 μM, which is 4.4-fold more potent than the lead compound **4** and 3.6-fold more potent than the cinnamic acid hydroxamate **1** (IC_{50} = 8.9 μM, FRET-based assay). Compound **1** has been used as a positive control in our assay. The IC_{50} value reported here for compound **1** is higher than the original reported value (IC_{50} = 0.41 μM),[16] and similar differences have also been observed by other laboratories.[17,22] The difference between these values is probably due to the use of different forms of the SNAP-25 substrate or different concentrations of enzyme. Assay conditions (temperature and incubation time) may also be partly or wholly responsible for these discrepant values.

Almost all of the active type I inhibitors are more selective for BoNT/A LC, as indicated by poorer anthrax LF inhibitory activity. Compounds **12** and **15** were the most selective BoNT/A LC inhibitors, demonstrating over 10-fold selectivity versus the LF. The most potent type II inhibitor, compound **44a,** also exhibited more than 5-fold selectivity for BoNT/A LC versus anthrax LF. Moreover, no inhibitory activities were observed for compounds **12** and **44a** against metalloproteases BoNT/B, human MMP-1 and MMP-9 (data not shown), further demonstrating the high specificity of these compounds for BoNT/A LC.[30]

Molecular Modeling. Several X-ray structures of BoNT/A LC complexed with small peptides or small molecules are now available, and they have revealed an unexpected conformational flexibility in the enzyme active site.[26,27,31,32] To better understand the binding mode and rationalize the improved potency of the 2-(phenoxyphenyl)indole series of compounds (type I derivatives), we performed a molecular modeling study with compound **12** and BoNT/A LC. Realizing that all of the four basic moieties of compound **12** may be ionized at physiological pH and that combinations of ionized species can exist in the aqueous physiological solution, four ionized states (mono-, di-, tri- and tetraionized states) of compound **12** were first generated by the Schrödinger Epik program. These states were then docked into the BoNT/A LC active site along with the free base form. The +4 positively charged state showed the highest docking score.

Table 1. Inhibitory Activities of Type I Analogues against BoNT/A LC and LF Enzymes

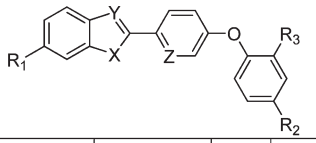

Compd. No.	R_1	R_2	R_3	X	Y	Z	BoNT/A IC_{50} (μM)[a,c]	[b]LF IC_{50} (μM)[b]
5	$C(=NH)NH_2$	$C(=NH)NH_2$	H	NH	CH	CH	11 (17)	35
9	CN	CN	H	NH	CH	CH	>100	n.d.[d]
10	$CONH_2$	$CONH_2$	H	NH	CH	CH	>100	>100
11	$C(=NH)NH_2$	CN	H	NH	CH	CH	>25	>100
12	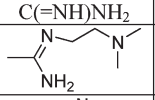	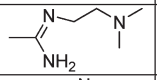	H	NH	CH	CH	2.5 (4.4)	28
13			H	NH	CH	CH	12.5 (9.4)	43
14			H	NH	CH	CH	21 (43)	>100
15	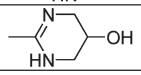	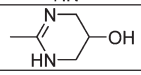	H	NH	CH	CH	7.3	>100
23a	CN	CN	H	NH	CH	N	>100	>100
23b	CN	CN	Cl	NH	CH	CH	>100	n.d.[d]
24a			H	NH	CH	N	69 (>100)	55
24b			H	NH	CH	N	67 (>100)	>100
24c		CN	Cl	NH	CH	CH	30	>100
25a			H	S	CH	CH	7.1 (25)	18
25b			H	S	CH	CH	54	>100
29		Cl	Cl	NH	CH	CH	>25 (52)	>100
32	Cl		H	NH	CH	CH	>100	51
35a			H	NH	N	CH	24.5	n.d.[d]
35b			H	NH	N	CH	28 (41)	n.d.

[a] Data represent an average value of two experiments in a FRET-based assay with variation less than 10%. [b] Data obtained by a FRET-based assay. [c] Data (in parentheses) represent average value of two experiments in a HPLC-based assay with variation less than 10%. [d] Compound shows strong fluorescence, so an accurate value was not determined.

To better account for the protein flexibility, the best conformations of each ionized state of the inhibitor were energy minimized in the bound state, with no restriction of the protein structure within 8 Å from the bound ligand. Further relative free binding energy calculations suggested that the +4 positively charged state is predominantly populated in the binding complexes in aqueous solution. The lowest energy binding mode of the +4 positively charged state is shown in Figure 3. The two protonated amidine moieties form hydrogen bonds or ionic interactions with Asp370 and Pro239. One of the amidine groups is hydrogen-bonded with a structural water molecule, and one of the protonated *N*,*N*-dimethylamino moieties is buried in a hydrophilic site surrounded by Thr214, Glu351, Asn362, and Arg363. The other *N*,*N*-dimethylamino moiety points toward the solvent accessible region, which may produce a favorable solvation binding energy. Moreover, the indole NH is hydrogen-bonded with the main chain carbonyl oxygen atom of Glu257, which further enhances the ligand binding affinity. Compared to the proposed binding mode of **5** reported earlier,[20,21] the overall more favorable binding mode of compound **12** in the BoNT/A LC active site may provide a molecular basis for the improvement of potency.

Interestingly, compound **12** apparently does not directly coordinate with the Zn ion, which is consistent with the finding that the inhibitory activity of compound **12** is independent of the Zn concentration (data not shown). Replacing the indole core of compounds **13** and **14** with

Table 2. Inhibitory Activities of Type II Analogues against BoNT/A LC and LF Enzymes

Compd. No.	R_1	R_2	X	Y	BoNT/A IC_{50} (μM)[a,c]	LF IC_{50} (μM)[b]
39	CN	F	NH	CH	>100	>100
40a	$CONH_2$	F	NH	CH	>100	>100
40b	$C(=NH)NH_2$	F	NH	CH	>100	48
40c		F	NH	CH	>100	40
43a	$CONH_2$	OCH_3	NH	CH	>100	>100
43b	$C(=NH)NH_2$	OCH_3	NH	CH	>100	>100
43c		OCH_3	NH	CH	45	61
44a			NH	CH	20	49
44b			NH	CH	>100	>100
46a			S	CH	43 (28)	>100
46b			S	CH	>100	n.d.[d]
49	$CONH_2$	F	S	N	>100	>100
50		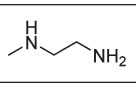	S	N	56	>100

[a] Data represent an average value of two experiments in a FRET-based assay with variation less than 10%. [b] Data obtained by a FRET-based assay. [c] Data (in parentheses) represent average value of two experiments in a HPLC-based assay with variation less than 10%. [d] Compound shows strong fluorescence, so an accurate value was not determined.

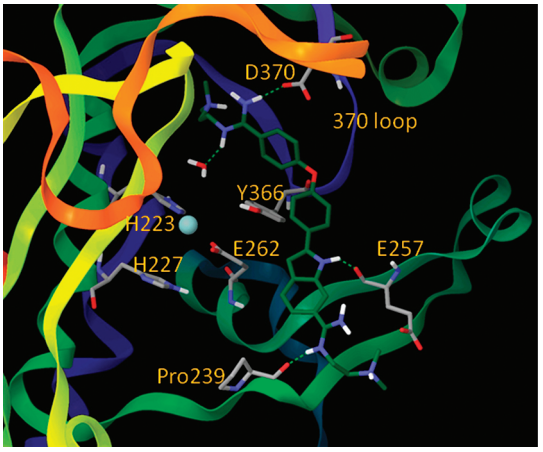

Figure 3. Proposed binding mode for type I inhibitor **12** (shown in a green stick model). Oxygen atoms are red, nitrogen atoms are blue, hydrogen atoms are white, and Zn is cyan. BoNT/A LC is displayed as a ribbon structure.

the similarly hydrophobic benzothiophene core, e.g., compounds **25a** and **25b**, improves the inhibitory activity for BoNT/A LC. However, replacement of the indole core with the more basic and hydrophilic benzimidazole core, e.g., compounds **35a** and **35b**, gives lower affinity compounds for BoNT/A LC. Additionally, replacement of the central phenyl ring with a basic pyridyl ring also leads to decreased inhibitory activity for the BoNT/A LC, e.g., for compounds **24a** and **24b**. The proposed binding mode also suggests that small substituents on the scaffold may be tolerated. Compounds **24c** and **29**, which contain substituents on the phenoxy ring, both maintain inhibitory activity for BoNT/A LC.

Conclusion

To optimize the potency of the lead compound **5**, we have synthesized two series of compounds with three-ring or two-ring scaffolds using various synthetic methods. The biological activities of the two series of compounds have been evaluated in FRET-based BoNT/A LC and anthrax LF assays. Structure−activity relationship studies have demonstrated that basic groups on both ends of the scaffolds are necessary for potency and that additional hydrogen-bonding or ionic interactions may be incorporated by adding polar or basic substitutions to the amidine moieties. Hydrophobic cores, e.g., indole or benzothiophene cores, are required for interaction with the enzyme active site, whereas polar atom replacement in the phenyl linker may alter the electronic environment to ultimately decrease potency. The SAR that we have identified will help to further optimize existing leads and allow the design of new small molecule BoNT/A LC inhibitors. The optimization effort has led to the identification of a potent BoNT/A LC inhibitor **12**, which displays an IC_{50} value of 2.5 μM in the BoNT/A LC assay, is 4.4-fold more potent than the original lead compound **5**, and is 3-fold more potent than the cinnamic acid hydroxamate **1** (IC_{50} = 8.9 μM, FRET assay). Moreover, compound **12** also showed cellular activity in a chick neuronal assay.[30] Compound **12** is highly specific, is 10-fold more selective over the metalloprotease anthrax LF, and does not inhibit BoNT/B LC, human metalloprotease MMP-1 or MMP-9.[26] In summary, we have discovered a potent, highly specific lead candidate that may be suitable for further development as a therapeutic agent for BoNT/A LC, which is a bioterrorist threat of increasing importance.

Experimental Section

General Procedures. All commercially obtained solvents and reagents were used as received. Melting points were determined

in open capillary tubes with an EZ-Melt (Stanford Research Systems) apparatus and are uncorrected. ^{1}H NMR spectra were determined on a Bruker 300 MHz instrument. Chemical shifts are given in δ values referenced to the internal standard tetramethylsilane. LC−MS analyses were performed by CreaGen Biosciences, Inc. (Woburn, MA) using a Shimadzu LC-10 AD VP HPLC, with Waters micromass quattro ultima triple-quad MS. High resolution mass spectra were recorded on an Agilent LC/MSD TOF high accuracy instrument at Scripps Research Institute. Elemental analyses were performed by Columbia Analytical Services. All of the compounds tested in vitro showed >95% purity by LC−MS except compounds **23b** (93%) and **24c** (90%).

4-(4-Formylphenoxy)benzonitrile (7). 4-Hydroxybenzaldehyde (**6**, 5.04 g, 41.3 mmol), 4-fluorobenzonitrile (5.0 g, 41.3 mmol), and K_2CO_3 (5.8 g, 42 mmol) were mixed in DMF (35 mL) and heated to 150−160 °C using a heating mantle. After 3 h the reaction mixture was cooled, and 2 N NaOH solution (150 mL) was added followed by ice−water (200 mL). The product precipitated and was collected by filtration and dried to give a brown solid (8.0 g, 87% yield). R_f = 0.30 (3:1 hexane/EtOAc), mp = 94−95 °C; ^{1}H NMR (300 MHz, DMSO-d_6) δ 9.91 (s, 1H), 7.92 (d, J = 8.4 Hz, 4 H), 7.85 (d, J = 8.5 Hz, 4H), 7.22 (d, J = 3.7 Hz, 4H), 7.19 (d, J = 3.6 Hz, 4H).

(*E*)-1-(4-Cyano-2-nitrophenyl)-2-(4-(4-cyanophenoxy)phenyl)-ethene (8). 4-Methyl-3-nitrobenzonitrile (5.08 g, 31.4 mmol) and 4-(4-formylphenoxy)benzonitrile (7.0 g, 31.4 mmol) were heated together to 150 °C until the compounds melted. Sulfolane (8 mL) and piperidine (1.5 mL) were added and the resulting solution was stirred at 150 °C for 4 h and cooled to room temperature to yield a yellow solid (7.74 g, 67% yield) after collection and drying. R_f = 0.15 (4:1 hexane/EtOAc), mp = 193−194 °C; ^{1}H NMR (300 MHz, DMSO-d_6) δ 8.55 (s, 1H), 8.20 (s, 2H), 7.87 (d, J = 8.7 Hz, 2H), 7.75 (d, J = 8.4 Hz, 2H), 7.59 (d, J = 16.0 Hz, 1H), 7.44 (d, J = 16.0 Hz, 1H), 7.21 (d, J = 9.8 Hz, 2H), 7.18 (d, J = 9.0 Hz, 2H).

2-(4-(4-Cyanophenoxy)phenyl)indole-6-carbonitrile (9). Compound **8** (5.0 g, 13.6 mmol) was suspended in triethyl phosphite (30 mL) and heated to reflux using a heating mantle for 1 h. The solution was cooled to room temperature and excess triethyl phosphite was removed by distillation under vacuum. The residue was purified by flash chromatography using 25% ethyl acetate in hexane to yield a light-yellow solid **9** (2.5 g, 55% yield): R_f = 0.21 (3:1 hexane/EtOAc), mp = 254−256 °C; ^{1}H NMR (300 MHz, DMSO-d_6) δ 12.17 (s, 1H), 8.02 (d, J = 8.6 Hz, 2H), 7.88 (d, J = 8.5 Hz, 2H), 7.84 (s, 1H), 7.71 (d, J = 8.2 Hz, 1H), 7.35 (dd, J = 0.7, 8.3 Hz, 1H), 7.30 (d, J = 8.6 Hz, 2H), 7.20 (d, J = 8.5 Hz, 2H), 7.08 (s, 1H).

2-(4-(4-Carbamoylphenoxy)phenyl)-1*H*-indole-6-carboxamide (10). Compound **9** (130 mg, 0.39 mmol) was dissolved in CH_2Cl_2/hexanes (16 mL, 1:1), and concentrated H_2SO_4 (8 mL) was added at 0 °C. The resulting solution was stirred for 24 h and poured onto ice (20 g). EtOAc (10 mL) was added, and the precipitates were collected and washed with H_2O to obtain a light-yellow solid **5** (119 mg, 83% yield). R_f = 0.11 (1:9 MeOH/$CHCl_3$), mp = 170−171 °C; ^{1}H NMR (300 MHz, DMSO-d_6) δ 11.78 (s, 1H), 7.97−7.92 (m, 7H), 7.53 (m, 2H), 7.32 (s, 1H), 7.20 (d, J = 8.5 Hz, 2H), 7.19 (s, 1H), 7.10 (d, 8.5 Hz, 2H), 6.93 (s, 1H). Anal. Calcd for $C_{22}H_{17}N_3O_3 \cdot 0.8H_2O$: C, 68.49; H, 4.86; N, 10.89. Found: C, 68.52; H; 4.68; N, 10.84.

2-(4-(4-Cyanophenoxy)phenyl)-1*H*-indole-6-carboximidamide Hydrochloride Salt (11). Compound **9** (200 mg, 0.60 mmol) was dissolved in THF (10 mL) at room temperature, and LiN(TMS)$_2$ (1.0 g, 6.0 mmol) was added. The resulting solution was stirred overnight, after which time TLC showed the disappearance of the starting material. The reaction solution was poured over ice, and the precipitated solid was washed with cold water. The crude product was dissolved in a minimum amount of MeOH and treated with 2 M HCl in diethyl ether, and the diamidine HCl salt was precipitated, filtered, and dried to give compound **11** (176 mg, 83%). R_f = 0.11 (80:18:2 $CHCl_3$/CH_3OH/CH_3NH_2), mp = 198−199 °C; ^{1}H NMR (300 MHz, DMSO-d_6) δ 7.98 (d, J = 8.8 Hz, 2H), 7.84 (d, J = 8.5 Hz, 2H), 8.31 (s, 1H), 7.69 (d, J = 8.3 Hz, 1H), 7.32 (dd, J = 1.4, 8.2 Hz, 1H), 7.18 (d, J = 8.8 Hz, 2H), 7.09 (d, J = 8.8 Hz, 2H), 7.03 (s, 1H). HRMS (ESI-TOF) m/z calcd for $C_{22}H_{17}N_4O$ 353.1402 (M + H)$^+$, found 353.1401.

***N*′-(2-(Dimethylamino)ethyl)-2-(4-(4-(*N*′-2-(dimethylamino)-ethyl)carbamimidoyl)phenoxy)phenyl)-1*H*-indole-6-carboximidamide (12).** Compound **9** (200 mg, 0.6 mmol) was gently stirred in anhydrous ethanol (50 mL) at 0 °C, and HCl gas was purged into the solution until saturation occurred. The resulting solution was stirred at room temperature for 2 days (reaction bottle was capped tightly), and the solvent and HCl were evaporated to dryness. To the residue dissolved in anhydrous ethanol (20 mL) was added *N*,*N*-dimethylethylenediamine (526 mg, 6.0 mmol), and the resulting solution was stirred at room temperature for 24 h. The reaction mixture was evaporated at 35 °C and dried at room temperature under high vacuum for 24 h to give a crude product, which was purified by reverse phase HPLC on a C-18 column using a 21 min method with a gradient of 10−60% acetonitrile−H_2O to give the title compound (143 mg, yield 25%). Mp = 92−93 °C; ^{1}H NMR (DMSO-d_6) δ 12.29 (s, 1H), 10.25 (br, 2H), 9.81 (br, 1H), 9.72−9.66 (m, 3H), 9.28 (s, 1H), 9.14 (s, 1H), 8.06 (d, J = 8.7 Hz, 2H), 7.89 (s, 1H), 7.86 (d, J = 1.8 Hz, 2H), 7.75 (d, J = 8.4 Hz, 1H), 7.43 (dd, J = 9. 1.2 Hz, 4H), 7.08 (s, 1H), 3.83 (br, 4H), 3.45 (d, J = 6.3 Hz, 4H), 2.91 (s, 6H), 2.89 (s, 6H). LC−MS (+ESI): m/z 512.5 (M + H)$^+$. HPLC t_R = 10.01 min. Anal. Calcd for $C_{30}H_{37}N_7O \cdot 4TFA \cdot H_2O$: C, 46.30; H, 4.40; N, 9.95. Found: C, 46.06; H, 4.40; N, 9.68.

6-(4,5-Dihydro-1*H*-imidazol-2-yl)-2-(4-(4-(4,5-dihydro-1*H*-imidazol-2-yl)phenoxy)phenyl)-1*H*-indole (13). Compound **9** (153 mg, 0.46 mmol) and P_2S_5 (55.6 mg, 0.25 mmol) were dissolved in ethylenediamine (3 mL) in a sealed tube, and the tube was heated to 120 °C in an oil bath for 2 h. The tube was cooled to room temperature, and the green solution was poured into water (90 mL). After 15 min the solids were collected and rinsed with cold water to give **13** as an off-white solid (195 mg, 93% yield). R_f = 0.09 (80:18:2 $CHCl_3$/CH_3OH/CH_3NH_2), mp = 290−291 °C; ^{1}H NMR (300 MHz, DMSO-d_6) δ 11.75, 7.94 (d, J = 7.1 Hz, 2H), 7.87 (s, 1H), 7.86 (d, J = 7.1 Hz, 1H), 7.85 (d, J = 8.8 Hz, 2H), 7.53 (s, 2H), 7.17 (d, J = 8.8 Hz, 2H), 7.10 (d, J = 6.9 Hz, 1H), 7.09 (d, J = 8.8 Hz, 2H), 6.90 (s, 1H), 3.63 (s, 4H), 3.60 (s, 4H). HRMS (ESI-TOF) m/z calcd for $C_{26}H_{24}N_5O$ 422.1981 (M + H)$^+$, found 422.1979.

6-(1,4,5,6-Tetrahydropyrimidin-2-yl)-2-(4-(4-(1,4,5,6-tetrahydropyrimidin-2-yl)phenoxy)phenyl)-1*H*-indole (14). Compound **9** (400 mg, 1.20 mmol) and P_2S_5 (133 mg, 0.59 mmol) were dissolved in 1,3-diaminopropane (15 mL) in a sealed tube. The tube was heated to 120 °C in an oil bath for 2 h. After cooling to room temperature, the green solution was poured into water (100 mL) and after 15 min the solids were collected and rinsed with cold water to give **14** as a white solid (526 mg, 98% yield). Mp = 183−184 °C; ^{1}H NMR (300 MHz, DMSO-d_6) δ 8.03 (d, J = 8.7 Hz, 2H), 7.85 (s, 1H), 7.81 (d, J = 8.7 Hz, 2H), 7.67 (d, J = 8.4 Hz, 1H), 7.36 (dd, J = 1.2, 9.0 Hz, 1H), 7.18 (d, J = 8.7 Hz, 2H), 7.1 (d, J = 8.7 Hz, 2H), 6.99 (s, 1H), 3.49 (t, J = 5.4 Hz, 4H), 3.39 (t, J = 5.7 Hz, 4H), 1.95 (t, J = 4.2 Hz, 2H), 1.78 (t, J = 5.1 Hz, 2H). HRMS (ESI-TOF) m/z calcd for $C_{28}H_{28}N_5O$ 450.2294 (M + H)$^+$, found 450.2281.

2-(4-(4-(6-(5-Hydroxy-1,4,5,6-tetrahydropyrimidin-2-yl)-1*H*-indol-2-yl)phenoxy)phenyl)-1,4,5,6-tetrahydropyrimidin-5-ol (15). Compound **9** (200 mg, 0.6 mmol), phosphorus pentasulfide (66 mg, 0.3 mmol), and 2-hydroxy-1,3-diaminopropane (2 g) were stirred at 120 °C under nitrogen in a sealed tube for 2 h. The reaction mixture was cooled to room temperature and poured into excess water and was stirred for 15 min and the resulting gray precipitate was collected by filtration and air-dried to give **15** (241 mg, 84%). Mp = 223−224 °C; ^{1}H NMR (300 MHz, DMSO-d_6) δ 12.64 (br, 1H), 8.06 (d, J = 8.1 Hz, 2H), 7.89

(s, 1H), 7.84 (d, J = 8.4 Hz, 2H), 7.68 (d, J = 8.1 Hz, 1H), 7.38 (d, J = 8.4 Hz, 1H), 7.16 (dd, J = 8.7, 21 Hz, 4H), 7.00 (s, 1H), 4.20 (s, 1H), 3.99 (s, 1H), 3.57−3.35 (m, 7H), 3.23 (dd, J = 4.5, 12 Hz, 3H). Anal. Calcd for $C_{28}H_{27}N_5O_3 \cdot 2CF_3COOH \cdot 1.5H_2O$: C, 52.18; H, 4.38; N, 9.51. Found: C, 52.10; H; 4.19; N, 9.57.

4-(4-Bromophenoxy)benzonitrile (19a). 4-Bromophenol (**17a**, 4.0 g, 23.1 mmol) and 4-fluorobenzonitrile (**18a**, 2.8 g, 23.1 mmol) were heated together to 150 °C until the compound melted. Piperidine (1.0 mL) was added, and the resulting solution was stirred at 150 °C for 4 h and cooled to room temperature. The precipitate was collected by filtration and washed with water to yield a red solid (5.2 g, 82% yield). R_f = 0.54 (1:9 EtOAc/hexane), mp = 78−79 °C; ^{1}H NMR (300 MHz, DMSO-d_6) δ 7.86 (d, J = 8.7 Hz, 2H), 7.65 (d, J = 8.7 Hz, 2H), 7.16−7.11 (m, 4H).

2-Bromo-5-(4-cyanophenoxy)pyridine (19b). Compound **19b** was prepared in the same fashion as for **19a** and was obtained as white solid. Mp = 118−119 °C; ^{1}H NMR (300 MHz, $CDCl_3$) δ 8.22 (d, 1H, J = 3 Hz), 7.67 (ddd, J = 2.4, 4.5, 14.1 Hz, 2H), 7.53 (d, J = 8.7 Hz, 1H), 7.28 (dd, J = 3, 8.7 Hz, 1H), 7.06 (ddd, J = 2.7, 4.8, 11.7 Hz, 2H).

1-Bromo-4-(2-chloro-4-cyanophenoxy)benzene (19c). Compound **19c** was prepared in the same fashion as for **19a** and was obtained as a white solid. Mp = 161−162 °C; ^{1}H NMR (300 MHz, $CDCl_3$) δ 7.95 (d, J = 2.4 Hz, 1H), 7.66 (dd, J = 2.1, 7.5 Hz, 1H), 7.49 (ddd, J = 3.3, 5.4, 12.3 Hz, 2H), 6.95 (d, J = 8.7 Hz, 1H), 6.89 (ddd, J = 3.3, 5.7, 12.3 Hz, 2H).

General Synthesis of 23a−c. A mixture of corresponding boronic acid **20** (1.0 g, 1 equiv), compound **19** (1 equiv), tetrakistriphenylphosphinepalladium (0.1 equiv), and sodium carbonate (2 equiv) in 10% ethanol in toluene (50 mL) was heated at reflux under argon for 4 h. The reaction mixture was cooled to room temperature and evaporated to dryness. The residue was dissolved in ethyl acetate, washed thrice with water, followed by brine, dried over magnesium sulfate, and evaporated to give the crude product. Recrystallization from toluene gave compounds **22a**, **22b**, and **23c**, respectively. Compound **22a** or **22b** (0.5 g, 1 equiv) was stirred in a mixture of trifluoroacetic acid (10 mL) and 4 N HCl in dioxane (2 mL) at room temperature for 1 h. The solvent was evaporated. The residue was dissolved in ethyl acetate, washed with potassium carbonate solution, water, and brine, and dried over magnesium sulfate, and the solvent was evaporated. The crude product was recrystallized to give **23a** or **23b**.

2-(5-(4-Cyanophenoxy)pyridin-2-yl)-1*H*-indole-6-carbonitrile (23a). Compound **23a** was obtained as a white solid. R_f = 0.20 (3:1 hexane/EtOAc), mp = 239−240 °C; ^{1}H NMR (300 MHz, DMSO-d_6) δ 12.25 (s, 1H), 8.59 (d, J = 2.7 Hz, 1H), 8.19 (d, J = 8.7 Hz, 1H), 7.91 (d, J = 1.8 Hz, 1H), 7.90 (d, J = 2.4 Hz, 2H), 7.77 (dd, J = 3.0, 11.4 Hz, 2H), 7.35 (dd, J = 1.2, 8.1, 1H), 7.28 (dd, J = 4.5, 6.3 Hz, 2H), 7.26 (s, 1H). HRMS (ESI-TOF) m/z calcd for $C_{21}H_{13}N_4O$ 337.1089 $(M + H)^+$, found 337.1091.

2-(4-(2-Chloro-4-cyanophenoxy)phenyl)-1*H*-indole-6-carbonitrile (23b). Compound **23b** was obtained as a white solid. Mp = 123−125 °C; ^{1}H NMR (300 MHz, DMSO-d_6) δ 12.14 (br, 1H), 8.13 (d, J = 2.1 Hz, 1H), 7.97 (d, J = 8.7 Hz, 2H), 7.89 (dd, J = 2.1, 6 Hz, 1H), 7.82 (s, 1H), 7.70 (d, J = 8.1 Hz, 1H), 7.34 (dd, J = 1.5, 6 Hz, 1H), 7.21−7.16 (m, 3H), 7.04 (s, 1H).

2-(4-(4-Cyanophenoxy)phenyl)benzo[*b*]thiophene-6-carbonitrile (23c). Compound **23c** was obtained as a white solid. Mp = 219−220 °C; ^{1}H NMR (300 MHz, DMSO-d_6) δ 8.61 (d, J = 0.6 Hz, 1H), 8.01 (d, J = 7.5 Hz, 2H), 7.92 (t, J = 4.2 Hz, 4H), 7.76 (dd, J = 1.2, 9.0 Hz, 1H), 7.28 (d, J = 8.7 Hz, 2H), 7.22 (d, J = 9.0 Hz, 2H).

6-(4,5-Dihydroimidazol-2-yl)-2-(5-(4-(4,5-dihydroimidazol-2-yl)phenoxy)pyridine-2-yl)indole (24a). The synthetic procedure used was the same as described for compound **13**. Compound **24a** was obtained as a light-brown solid. R_f = 0.01 (80:18:2 $CHCl_3/CH_3OH/CH_3NH_2$), mp ≥300 °C; ^{1}H NMR (300 MHz, DMSO-d_6) δ 11.91 (s, 1H), 8.48 (d, J = 2.4 Hz, 1H), 8.08 (d, J = 8.7 Hz, 1H), 7.93 (s, 1H), 7.88 (d, J = 9.0 Hz, 2H), 7.62 (dd, J = 3.0, 9.0 Hz, 1H), 7.54 (d, J = 11.7 Hz, 1H), 7.50 (dd, J = 1.2, 8.4 Hz, 1H), 7.16 (d, J = 8.7 Hz, 1H), 7.14 (s, 2H), 3.61 (br, 10H). HRMS (ESI-TOF) m/z calcd for $C_{25}H_{23}N_6O$ 423.1933 $(M + H)^+$, found 423.1920.

6-(3,4,5,6-Tetrahydropyrimidin-2-yl)-2-(4-(4-(3,2,5,6-tetrahydropyrimidin-2-yl)phenoxy)phenyl)indole (24b). The synthetic procedure used was the same as described for compound **14**. Compound **24b** was obtained as a light-yellow powder. Mp = 183−184 °C; ^{1}H NMR (300 MHz, DMSO-d_6) δ 8.03 (d, 2H), 7.85 (s, 1H), 7.81 (d, 2H), 7.67 (d, 1H), 7.36 (dd, 1H), 7.18 (d, 2H), 7.10 (d, 2H), 6.99 (s, 1H), 3.49 (t, 4H), 3.39 (t, 4H), 1.95 (t, 2H), 1.78 (t, 2H). HRMS (ESI-TOF) m/z calcd for $C_{27}H_{27}N_6O$ 451.2246 $(M + H)^+$, found 451.2227.

2-(4-(2-Chloro-4-cyanophenoxy)phenyl)-6-(4,5-dihydro-1*H*-imidazol-2-yl)indole (24c). The synthetic procedure used was the same as described for compound **13**. Compound **24c** was purified by a 10 min method by reverse phase HPLC using a C-18 column and isolated as a tan powder. Mp = 167−168 °C; ^{1}H NMR (300 MHz, DMSO-d_6) δ 12.3 (s, 1H), 8.15−8.11 (m, 1H), 8.05 (d, J = 5.1 Hz, 2H), 8.01 (s, 1H), 7.91 (dd, J = 1.8, 9 Hz, 1H), 7.72 (d, J = 8.4 Hz, 1H),7.58 (d, J = 8.1 Hz, 1H), 7.51 (s, 1H), 7.19−7.17 (m, 3H), 7.04 (s, 1H), 3.95 (s, 4H).

2-(4-(4-(6-(4,5-Dihydro-1*H*-imidazol-2-yl)benzo[*b*]thiophen-2-yl)phenoxy)phenyl)-4,5-dihydro-1*H*-imidazole (2TFA Salt) (25a). The synthetic procedure used was the same as described for compound **13**. Compound **25a** was treated with TFA to give the di-TFA salt. Mp = 147−148 °C; ^{1}H NMR (300 MHz, DMSO-d_6) δ 10.59 (d, J = 3.9 Hz, 2 H), 10.51 (d, J = 3.9 Hz, 2 H), 8.64 (s, 1H), 8.12−7.89 (m, 7H), 7.32 (dd, J = 4.5, 8.7 Hz, 4H), 4.04 (d, J = 14.4 Hz, 8H). HRMS (ESI-TOF) m/z calcd for $C_{26}H_{23}N_4OS$ 439.1593 $(M + H)^+$, found 439.1596.

2-(4-(4-(6-(1,4,5,6-Tetrahydropyrimidin-2-yl)benzo[*b*]thiophen-2-yl)phenoxy)phenyl)-1,4,5,6-tetrahydropyrimidine (25b). The synthetic procedure used was the same as used for compound **14**. Compound **25b** was obtained as a white solid. Mp = 239−240 °C; ^{1}HNMR (300 MHz, DMSO-d_6) δ 8.31 (s, 1H), 7.85−7.78 (m, 7H), 7.14 (d, J = 8.4 Hz, 2H), 7.08 (d, J = 8.7 Hz, 2H), 3.42−3.34 (m, 8H), 1.78−1.68 (m, 4H). HRMS (ESI-TOF) m/z calcd for $C_{28}H_{27}N_4OS$ 467.1906 $(M + H)^+$, found 467.1895.

1-(4-Bromophenoxy)-2,4-dichlorobenzene (27). The synthetic procedure used was the same as that used for compound **19c**. Compound **27** was obtained as a pale-brown oil. R_f = 0.76 (5% EtOAc/hexane); ^{1}H NMR (300 MHz, $CDCl_3$) δ 7.45 (d, 1H), 7.41 (dd, 2H), 7.19 (dd, 1H), 6.91 (d, 1H), 6.81 (dd, 2H).

***tert*-Butyl 6-Cyano-2-(4-(2,4-dichlorophenoxy)phenyl)-1*H*-indole-1-carboxylate (28).** A mixture of *N*-*tert*-butoxycarbonyl-6-cyanoindole-2-boronic acid **20a** (500 mg, 1.8 mmol), compound **27** (668 mg, 2.1 mmol), tetrakistriphenylphosphinepalladium (40 mg, 0.035 mmol), sodium carbonate (371 mg, 3.5 mmol) in 10% ethanol in toluene (18 mL) was heated at reflux under argon for 1.5 h. The reaction mixture was cooled to room temperature, washed thrice with water, followed by brine, and dried over magnesium sulfate, and the solvent was evaporated. The crude product was purified by flash chromatography using 8% EtOAc in hexane to obtain a light-yellow solid (411 mg, 49% yield). Mp = 122−124 °C; ^{1}H NMR (300 MHz, $CDCl_3$) δ 8.56 (br, 1H), 7.59 (d, J = 7.8 Hz, 1H), 7.49 (s, 2H), 7.38 (d, J = 8.7 Hz, 2H), 7.26 (dd, J = 2.4, 8.7 Hz, 1H), 7.03 (d, J = 8.7 Hz, 1H), 6.98 (d, J = 9 Hz, 2H), 6.58 (s, 1H), 1.37 (s, 9H).

2-(4-(2,4-Dichlorophenoxy)phenyl)-6-(4,5-dihydro-1*H*-imidazol-2-yl)-1*H*-indole (29). Compound **28** (15 mg, 0.31 mmol), phosphorus pentasulfide (17 mg, 0.078 mmol), and ethylenediamine (5 mL) were stirred at 120 °C under nitrogen in a sealed tube for 2 h. The reaction mixture was cooled to room temperature, poured into excess water, stirred for 15 min and the white precipitate was collected by filtration and dried in air to obtain an off-white powder (84.5 mg, 64% yield). R_f = 0.17 (80:18:2 $CHCl_3/CH_3OH/CH_3NH_2$), mp=219−220 °C; ^{1}H NMR

(300 MHz, DMSO-d_6) δ 11.71 (s, 1H), 7.91 (d, J = 9 Hz, 2H), 7.86 (s, 1H), 7.81 (d, J = 2.7 Hz, 1H), 7.52 (s, 2H), 7.47 (dd, J = 2.4, 8.7 Hz, 1H), 7.20 (d, J = 8.7 Hz, 1H), 7.10 (d, J = 8.7 Hz, 2H), 6.89 (s, 1H), 3.62 (s, 4H). LC−MS (+ESI): m/z 422.3 $(M + H)^+$. Anal. Calcd for $C_{23}H_{17}Cl_2N_3O \cdot 0.2H_2O$: C, 64.86; H, 4.12; N, 9.87. Found: C, 64.72; H; 4.11; N, 9.74.

***tert*-Butyl 6-Chloro-2-(4-(4-cyanophenoxy)phenyl)-1*H*-indole-1-carboxylate (31).** Compound **30** (1.0 g, 3.4 mmol), compound **19a** (1.11 g, 4.1 mmol), tetrakistriphenylphosphinepalladium (79 mg, 0.068 mmol), and sodium carbonate (742 mg, 7 mmol) in 10% ethanol in toluene (36 mL) were heated at reflux under argon for 1.5 h. The reaction mixture was cooled to room temperature, washed thrice with water, followed by brine, dried over magnesium sulfate, and the solvent was evaporated. The crude product was purified by flash chromatography using 1:1 dichloromethane/hexane to obtain a light-yellow solid (604 mg, 40% yield). Mp = 148−149 °C; ^{1}H NMR (300 MHz, $CDCl_3$) δ 8.3 (s, 1H), 7.64 (d, J = 9.0 Hz, 2H), 7.46 (dd, J = 3.0, 9.0 Hz, 3H), 7.24 (dd, J = 3.0, 9.0 Hz, 1H), 7.09 (t, J = 9.0 Hz, 4H), 6.53 (s, 1H), 1.39 (s, 9H).

6-Chloro-2-(4-(4-(4,5-dihydro-1*H*-imidazol-2-yl)phenoxy)-phenyl)-1*H*-indole (32). Compound **31** (15 mg, 3.4 mmol), phosphorus pentasulfide (19 mg, 0.084 mmol), and ethylenediamine (5 mL) were stirred at 120 °C under nitrogen in a sealed tube for 2 h. The reaction mixture was cooled to room temperature and poured into excess water, stirred for 15 min and the resulting precipitate was collected by filtration and dried in air to give a white solid (84.9 mg, 65% yield). R_f = 0.17 (80:18:2 $CHCl_3/CH_3OH/CH_3NH_2$), mp = 271−272 °C; ^{1}H NMR (300 MHz, DMSO-d_6), δ 11.69 (s, 1H), 7.89 (d, J = 8.7 Hz, 2H), 7.86 (d, J = 8.7 Hz, 2H), 7.54 (d, J = 9.0 Hz, 1H), 7.39 (d, J = 1.5 Hz, 1H), 7.17 (d, J = 9.0 Hz, 2H), 7.09 (d, J = 9.0 Hz, 2H), 7.01 (dd, J = 1.8, 8.4 Hz, 1H), 6.85 (d, J = 1.5 Hz, 1H), 3.6 (s, 4H). HRMS (ESI-TOF) m/z calcd for $C_{23}H_{19}ClN_3O$ 388.1217 $(M + H)^+$, found 388.1208.

2-(4-(4-Cyanophenoxy)phenyl)-1*H*-benzo[*d*]imidazole-6-carbonitrile (34). A mixture of 3,4-diaminobenzonitrile (**33**, 500 mg, 3.8 mmol), 4-(4-cyanophenoxy)benzaldehyde (**7**, 848 mg, 3.8 mmol), and 40% aqueous sodium bisulfite (2.2 mL, 8.3 mol) in ethanol (20 mL) was stirred at 80 °C for 19 h. A white precipitate appeared. The supernatant dark-brown solution was decanted and evaporated to dryness. The crude product was washed twice with hot toluene to give a white solid (1.31 g, 100%). Mp = 222−223 °C; ^{1}H NMR (300 MHz, DMSO-d_6) δ 8.36 (d, J = 8.7 Hz, 2H), 8.21 (s, 1H), 7.97 (d, J = 8.4 Hz, 2H), 7.83 (d, J = 8.4 Hz, 1H), 7.66 (d, J = 8.4 Hz, 1H), 7.39 (d, J = 8.4 Hz, 2H), 7.31 (d, J = 8.4 Hz, 2H). LC−MS (+ESI): m/z 336.3 (M^+).

6-(4,5-Dihydro-1*H*-imidazol-2-yl)-2-(4-(4-(4,5-dihydro-1*H*-imidazol-2-yl)phenoxy)phenyl)-1*H*-benzo[*d*]imidazole (35a). The synthetic procedure used was the same as used for compound **13**. Compound **35a** was obtained as a gray powder. Mp = 257−260 °C; ^{1}H NMR (300 MHz, DMSO-d_6) δ 8.26 (d, J = 9.0 Hz, 2H), 8.15 (s, 1H), 7.91 (d, J = 9.0 Hz, 2H), 7.77 (dd, J = 1.5, 8.4 Hz, 1H), 7.69 (d, J = 8.4 Hz, 1H), 7.24 (d, J = 9 Hz, 2H), 7.18 (d, J = 8.7 Hz, 2H), 3.82 (s, 4H), 3.67(s, 4H). LC−MS (+ESI): m/z 423.43 $(M + H)^+$.

6-(1,4,5,6-Tetrahydropyrimidin-2-yl)-2-(4-(4-(1,4,5,6-tetrahydropyrimidin-2-yl)phenoxy)phenyl)-1*H*-benzo[*d*]imidazole (35b). The synthetic procedure used was the same as used for compound **14**. Compound **35b** was obtained as a white solid. Mp = 247−250 °C; ^{1}H NMR (300 MHz, DMSO-d_6) δ 8.27 (d, J = 8.7 Hz, 2H), 7.89 (s, 1H), 7.78 (d, J = 8.7 Hz, 2H), 7.53 (d, J = 9 Hz, 1H), 7.38 (d, J = 8.1 Hz, 1H), 7.11 (d, J = 8.7 Hz, 2H), 7.06 (d, J = 8.7 Hz, 2H), 3.45 (t, J = 5.5 Hz, 4H), 3.36 (t, J = 5.4 Hz, 4H), 1.89 (t, J = 5.4 Hz, 2H), 1.72 (t, J = 5.4 Hz, 2H). HRMS (ESI-TOF) m/z calcd for $C_{27}H_{27}N_6O$ 451.2246 $(M + H)^+$, found 451.2247.

(*E*)-1-(4-Fluorophenyl)-2-(4-cyano-2-nitrophenyl)ethene (38). 4-Methyl-3-nitrobenzonitrile (**36**, 4.0 g, 24.7 mmol) and 4-fluorobenzaldehyde (**37**, 3.06 g, 24.7 mmol) were heated together to 150 °C until melt occurred. Piperidine (1.23 mL) was added, and the resulting solution was stirred at 150 °C for 4 h. After the mixture was cooled to room temperature, cold MeOH was added to the residue, and filtration yielded a red solid (6.2 g, 96% yield). R_f = 0.43 (3:1 hexane/EtOAc), mp = 137−138 °C; ^{1}H NMR (300 MHz, DMSO-d_6) δ 8.26 + 8.19 (2d, J = 1.6, 1.7 Hz, 1H), 7.90 (d, J = 8.2 Hz, 1H), 7.84 + 7.75 (2dd, J = 1.6, 17.2, Hz, 1H), 7.57−7.39 (m, 3H), 7.22 + 7.7.15 (2d, J = 5.9, 6.4 Hz, 1H), 7.09 + 6.90 (2d, J = 8.6, 8.9 Hz, 1H).

2-(4-Fluorophenyl)-1*H*-indole-6-carbonitrile (39). Compound **38** (6.0 g, 22.4 mmol) was suspended in triethyl phosphite (70 mL) and heated to 150−160 °C for 1.5 h. The reaction mixture was cooled to room temperature and excess triethyl phosphite was removed by distillation under vacuum. The residue was recrystallized from methanol to give an off-white solid (**39**, 2.4 g, 45% yield): R_f = 0.44 (3:1 hexane/EtOAc), mp = 110−111 °C; (300 MHz, DMSO-d_6) δ 12.15 (s, 1H), 8.00−7.95 (m, 2H), 7.83 (s, 1H), 7.71 (d, J = 8.3 Hz, 1H), 7.40−7.33 (m, 3H), 7.06 (s, 1H).

2-(4-Fluorophenyl)-1*H*-indole-6-carboxamide (40a). The synthetic procedure used was the same as used for compound **10**. Compound **40a** was obtained as a gray solid. R_f = 0.51 (80:18:2 $CHCl_3/CH_3OH/CH_3NH_2$), mp = 236−237 °C; ^{1}H NMR (300 MHz, DMSO-d_6) δ 11.79 (s, 1H), 7.95 (t, J = 6.0 Hz, 4H), 7.55 (s, 2H), 7.34 (t, J = 8.8 Hz, 2H), 7.19 (s, 1H), 6.94 (s, 1H). HRMS (ESI-TOF) m/z calcd for $C_{15}H_{12}FN_2O$ 255.0934 $(M + H)^+$, found 255.0927.

2-(4-Fluorophenyl)-1*H*-indole-6-carboximidamide (40b). The synthetic procedure used was similar to that used for compound **12**. Compound **40b** was obtained as a green powder. Mp = 262−263 °C; ^{1}H NMR (300 MHz, DMSO-d_6) δ 9.2−8.6 (br, 4H), 7.99 (dd, 2H), 7.88 (s, 1H), 7.69 (d, 1H), 7.40 (d, 1H), 7.33 (t, 2H), 7.02 (s, 1H). HRMS (ESI-TOF) m/z calcd for $C_{15}H_{13}FN_3$ 254.1094 $(M + H)^+$, found 254.1091.

6-(4,5-Dihydro-1*H*-imidazol-2-yl)-2-(4-fluorophenyl)-1*H*-indole (40c). The synthetic procedure used was the same as used for compound **13**. Compound **40c** was obtained as a light-brown solid. R_f = 0.01 (80:18:2 $CHCl_3/CH_3OH/CH_3NH_2$), mp = 227−228 °C; ^{1}H NMR (300 MHz, DMSO-d_6) δ δ 11.71 (s, 1H), 7.94 (d, J = 5.4 Hz, 1H), 7.91 (d, J = 5.4 Hz, 1H), 7.86 (s, 1H), 7.52 (s, 2H), 7.32 (t, J = 8.7 Hz, 2H), 6.91 (s, 1H), 6.7 (br, 1H), 3.61 (s, 4H). HRMS (ESI-TOF) m/z calcd for $C_{17}H_{15}FN_3$ 280.1250 $(M + H)^+$, found 280.1241.

***tert*-Butyl 6-Cyano-2-(4-methoxyphenyl)-1*H*-indole-1-carboxylate (42a).** The synthetic procedure used was the same as used for compound **23a**. Compound **42a** was obtained as a white solid. Mp = 206−207 °C; ^{1}H NMR (300 MHz, $CDCl_3$) 8.59 (s, br, 1H), 7.69 (d, J = 0.6 Hz, 1H), 7.64−7.60 (m, 3H), 7.34 (dd, J = 1.2, 1.5 Hz, 1H), 7.00 (dd, J = 0.9, 2.1 Hz, 2H), 6.76 (dd, J = 0.9, 2.1 Hz, 1H), 3.87 (s, 3H). LC−MS (+ESI): m/z 249.2 $(M + H)^+$.

***tert*-Butyl 6-cyano-2-(4-cyanophenyl)-1*H*-indole-1-carboxylate (42b).** The synthetic procedure used was the same as used for compound **23a**. Compound **42b** was obtained as a white solid. Mp = 279−280 °C; ^{1}H NMR (300 MHz, $CDCl_3$) δ 8.57 (s, 1H), 7.74 (dd, J = 2.1, 6.0 Hz, 2H), 7.65 (dd, J = 0.6, 8.1 Hz, 1H), 7.55 (dd, J = 2.1, 6.0 Hz, 2H), 7.51 (d, J = 1.5 Hz, 1H), 6.68 (s, 1H), 1.37 (s, 9H). LC−MS (+ESI): m/z 344.1 $(M + H)^+$.

2-(4-Methoxyphenyl)-1*H*-indole-6-carboxamide (43a). The synthetic procedure used was the same as used for compound **10**. Compound **43a** was obtained as a tan powder. Mp = 258−259 °C; ^{1}H NMR (300 MHz, DMSO-d_6) δ 11.65 (s, 1H), 7.93 (s, 1H), 7.84 (d, J = 9.0 Hz, 3H), 7.52−7.13 (m, 4H), 7.05 (d, J = 9.0 Hz, 1H), 6.82 (s, 1H), 3.82 (s, 3H). HRMS (ESI-TOF) m/z calcd for $C_{16}H_{15}N_2O_2$ 267.1134 $(M + H)^+$, found 267.1124.

2-(4-Methoxyphenyl)-1*H*-indole-6-carboximidamide (43b). The synthetic procedure used was the same as used for compound **12**. Compound **43b** was obtained as a pale-yellow powder. R_f = 0.07 (80:18:2 $CHCl_3/CH_3OH/CH_3NH_2$), mp = 290−291 °C; ^{1}H

NMR (300 MHz, DMSO-d_6) δ 12.19 (br, 1H), 9.08 (br, 3H), 7.9 (d, J = 9 Hz, 3H), 7.68 (d, J = 8 Hz, 1H), 7.43 (dd, J = 1.5, 9.0 Hz, 1H), 7.08 (d, J = 6 Hz, 2H), 6.95 (s, 1H), 3.83 (s, 3H). HRMS (ESI-TOF) m/z calcd for $C_{16}H_{16}N_3O$ 266.1293 $(M + H)^+$, found 266.1293.

2-(4-Methoxyphenyl)-6-(4,5-dihydro-1*H*-imidazol-2-yl)-1*H*-indole (43c). The synthetic procedure used was the same as used for compound **13**. Compound **38c** was obtained as a light-yellow powder. R_f = 0.41 (80:18:2 $CHCl_3/CH_3OH/CH_3NH_2$), mp = 241−242 °C; ^{1}H NMR (300 MHz, DMSO-d_6) δ 11.63 (br, 1H), 7.85 (d, J = 5.1 Hz, 2H), 7.81 (s, 1H), 7.49 (s, 2H), 7.04 (d, J = 8.7 Hz, 2H), 6.8 (s, 1H), 3.81 (s, 3H), 3.61 (s, 4H). HRMS (ESI-TOF) m/z calcd for $C_{18}H_{18}N_3O$ 292.1450 $(M + H)^+$, found 292.1449.

6-(4,5-Dihydro-1*H*-imidazol-2-yl)-2-(4-(4,5-dihydro-1*H*-imidazol-2-yl)phenyl)-1*H*-indole (44a). The synthetic procedure used was the same as used for compound **13**. Compound **44a** was obtained as a light-yellow powder. R_f = 0.34 (80:18:2 $CHCl_3/CH_3OH/CH_3NH_2$), mp = 289−291°C; ^{1}H NMR (300 MHz, DMSO-d_6) δ 11.88 (s, 1H), 7.97−7.86 (m, 4H), 7.6−7.52 (m, 2H), 7.05 (s, 1H), 3.65 (d, J = 9.0 Hz, 8H). LC−MS (+ESI): m/z 330.4 $(M + H)^+$. Anal. Calcd for $C_{20}H_{19}N_5 \cdot 0.7H_2O$: C, 70.24; H, 6.01; N, 20.48. Found: C, 70.47; H; 5.73; N, 20.04.

6-(3,4,5,6-Tetrahydropyrimidin-2-yl)-2-(4-(3,4,5,6-tetrahydropyrimidin-2-yl)phenyl)-1*H*-indole (44b). The synthetic procedure used was the same as used for compound **14**. Compound **44b** was obtained as a light-yellow powder. R_f = 0.04 (80:18:2 $CHCl_3/CH_3OH/CH_3NH_2$), mp > 300 °C; ^{1}H NMR (300 MHz, DMSO-d_6) δ 8.03 (d, J = 8.4 Hz, 2H), 7.88 (d, J = 8.4 Hz, 2H), 7.86 (s, 1H), 7.69 (d, J = 8.4 Hz, 1H), 7.37 (dd, J = 1.5, 8.4 Hz, 1H), 7.12 (s, 1H), 3.48 (t, J = 5.7 Hz, 4H), 3.41 (t, J = 5.4 Hz, 4H), 1.96−1.93 (m, 2H), 1.79−1.76 (m, 2H). LC−MS (+ESI): m/z 358.3 $(M + H)^+$.

2-(4-Cyanophenyl)benzo[*b*]thiophene-6-carbonitrile (45). A mixture of 6-cyanobenzo[*b*]thiophen-2-ylboronic acid (**20b**, 1 g, 4.9 mol), 4-bromobenzonitrile (**41b**, 1.08 g, 5.9 mol), (2-biphenyl)-di-*tert*-butylphosphine (146 mg, 0.49 mmol), $Pd(OAc)_2$ (55 mg, 0.25 mmol), and K_2CO_3 (1.35 g, 9.8 mmol) in DMF (30 mL) was heated in a sealed tube under argon atmosphere at 100 °C for 4 h, cooled to room temperature, and poured into an excess of water. The precipitate obtained was collected by filtration, washed with water, and dried at 50 °C under vacuum. The product was further purified by trituration with hot MeOH to yield a light-tan powder (1.28 g, 90% yield). R_f = 0.49 (80:18:2 $CHCl_3/CH_3OH/CH_3NH_2$), mp = 262−263 °C; ^{1}H NMR (300 MHz, DMSO-d_6) δ 8.67 (s, 1H), 8.22 (s, 1H), 8.07−7.96 (m, 5H), 7.79 (dd, J = 1.5, 8.4 Hz, 1H).

2-(4-(6-(4,5-Dihydro-1*H*-imidazol-2-yl)benzo[*b*]thiophen-2-yl)-phenyl)-4,5-dihydro-1*H*-imidazole (46a). The synthetic procedure used was the same as used for compound **13**. Compound **46a** was obtained as a light-yellow powder. R_f = 0.41 (80:18:2 $CHCl_3/CH_3OH/CH_3NH_2$), mp > 300 °C; ^{1}H NMR (300 MHz, DMSO-d_6) δ 8.39 (s, 1H), 8.01 (s, 1H), 7.94−7.85 (m, 6H), 7.0 (br, 1H), 3.64 (d, J = 4.2 Hz, 8H). HRMS (ESI-TOF) m/z calcd for $C_{20}H_{19}N_4S$ 347.1330 $(M + H)^+$, found 347.1330.

2-(4-(6-(1,4,5,6-Tetrahydropyrimidin-2-yl)benzo[*b*]thiophen-2-yl)phenyl)-1,4,5,6-tetrahydropyrimidine (2TFA Salt) (46b). The synthetic procedure used was the same as used for compound **14**. Compound **46b** was obtained as a light-brown powder. R_f = 0.08 (80:18:2 $CHCl_3/CH_3OH/CH_3NH_2$), mp = 227−228 °C; ^{1}H NMR (300 MHz, DMSO-d_6) δ 10.09 (s, 4H), 8.47 (s, 1H), 8.25 (s, 1H), 8.11 (d, J = 8.4 Hz, 3H), 7.86 (d, J = 8.4 Hz, 2H), 7.72 (dd, J = 1.8, 8.4 Hz, 1H), 3.54 (br, 8H), 2.01 (br, 4H). HRMS (ESI-TOF) m/z calcd for $C_{22}H_{23}N_4S$ 375.1643 $(M + H)^+$, found 375.1642.

2-(5-Fluoro-2-pyridyl)-6-benzo[*b*]thiphenecarbonitrile (48). The synthetic procedure used was the same as used for compound **23c**. Compound **48** was obtained as a light-yellow powder. Mp = 228−229 °C; ^{1}H NMR (300 MHz, $CDCl_3$) δ 8.52 ((d, J = 3 Hz, 1H), 8.18 (s, 1H), 7.79−7.87 (m, 3H), 7.58 (dd, J = 1.5, 6 Hz, 1H), 7.51 (dd, J = 8.1, 16.8 Hz, 1H). LC−MS (+ESI): m/z 255.3 $(M + H)^+$.

2-(5-Fluoro-2-pyridyl)-6-benzo[*b*]thiophenecarboxamide (49). The synthetic procedure used was the same as used for compound **10**. Compound **49** was obtained as a light-yellow powder. Mp = 250−252 °C; ^{1}H NMR (300 MHz, DMSO-d_6) δ 8.64 (d, 1H, J = 2.7 Hz), 8.52 (s, 1H), 8.26−8.19 (m, 2H), 8.08 (br, 1H), 7.95−7.86 (m, 2H), 7.45 (br, 1H). HRMS (ESI-TOF) m/z calcd for $C_{14}H_{10}FN_2OS$ 273.0498 $(M + H)^+$, found 273.0495.

***N*^{1}-(6-(6-(4,5-Dihydro-1*H*-imidazol-2-yl)benzo[*b*]thiophen-2-yl)-pyridine-3-yl)ethane-1,2-diamine (50).** Compound **48** (220 mg, 0.87 m mol), phosphorus pentasulfide (48 mg, 0.22 mmol), and ethylenediamine (5 mL) were stirred at 120 °C under nitrogen in a sealed tube for 2 h. The reaction mixture was cooled to room temperature and poured into excess water, stirred for 15 min, and the precipitate was collected by filtration and dried in air. Purification by a 10 min method using reverse phase HPLC on a C-18 column gave **50** as a light-yellow solid (87 mg, 30%). Mp = 211−212 °C; ^{1}H NMR (300 MHz, DMSO-d_6) δ 10.59 (s, 2H), 8.56 (s, 1H), 8.07−7.94 (m, 6H), 7.86 (d, J = 8.7 Hz, 1H), 7.13 (dd, J = 2.7, 9.0 Hz, 1H), 4.04 (s, 4H), 3.42 (t, J = 6.3 Hz, 2H), 3.04 (t, J = 5.4 Hz, 2H). HRMS (ESI-TOF) m/z calcd for $C_{18}H_{20}N_5S$ 338.1439 $(M + H)^+$, found 338.1435.

BoNT/A LC FRET Assay. The BoNT/A LC FRET-based assay was originally developed by Schmidt.[23] Test compound, 20 μM SNAP-25 (aa 187−203) peptide substrate of sequence SNRTRIDEAN[DnpK]RA[daciaC]RML (Peptides International, Louisville, KY), and 10 ng of BoNT/A LC (List Biological Laboratories, Campbell, CA) were incubated at 37 °C for 40 min in the presence of buffer (50 mM HEPES−0.05% Tween, pH 7.4) in a volume of 100 μL. The reactions were stopped with acetic acid (0.5% [final]) prior to measuring the fluorescence of the cleaved substrate at 485 nm following excitation at 398 nm in a Molecular Devices (Sunnyvale, CA) plate reader. IC_{50} values were obtained by dose−response measurements.

Anthrax Lethal Factor FRET Assay. The anthrax lethal factor FRET-based assay was previously reported.[28] The reaction mixture contained 20 μM peptide substrate (KKVYPYPME) with a fluorogenic coumarin group at the N-terminus and a 2,4-dinitrophenyl (DNP) quenching group at the C terminus (Peptides International, Louisville, KY), LF (50 ng) (List Biological Laboratories), 20 mM HEPES, pH 8.2, 0.05% Tween-20, and the test compound. The assay mixture was incubated at 30 °C for 15 min. The reactions were stopped with acetic acid (0.5% [final]) prior to measuring the fluorescence of the cleaved substrate at 395 nm following excitation at 324 nm in the Molecular Devices plate reader. IC_{50} values were obtained by dose−response measurements.

Molecular Modeling. The molecular modeling study was performed with the Schrödinger computational software package (Schrödinger, Inc., New York). X-ray coordinates of BoNT/A LC (PDB code 2G7N) were used for this modeling study. The ionic states of compound **12** were generated by Epik, version 1.6. The docking study was performed with Glide 5.0, and energies were minimized by Macromodel. For each state of compound **12**, 10 solutions were generated and subsequently ranked according to the Glide score. The best poses of ionic charged states were further thoroughly energy minimized (rmsd = 0.05 Å), and the relative free binding energies were calculated according to the following equation: $\Delta E = E_{complex} - (E_{enzyme} + E_{ligand})$.

Acknowledgment. This work was supported by the National Institutes of Health/National Institute of Allergy and Infectious Diseases (Grant 5U01AI070430). The content of this publication does not necessarily reflect the views or policies of the Department of Health and Human Services. The authors thank CreaGen Biosciences, Inc. for the preparation of noncommercial starting material **20b** and for scale-up synthesis of compounds **9** and **39**.

References

(1) Burnett, J. C.; Henchal, E. A.; Schmaljohn, A. L.; Bavari, S. The evolving field of biodefence: therapeutic developments and diagnostics. *Nat. Rev. Drug Discovery* **2005**, *4*, 281–297.

(2) Paddle, B. M. Therapy and prophylaxis of inhaled biological toxins. *J. Appl. Toxicol.* **2003**, *23*, 139–170.

(3) Clarke, S. C. Bacteria as potential tools in bioterrorism, with an emphasis on bacterial toxins. *Br. J. Biomed. Sci.* **2005**, *62*, 40–46.

(4) Hicks, R. P.; Hartell, M. G.; Nichols, D. A.; Bhattacharjee, A. K.; van Hamont, J. E.; Skillman, D. R. The medicinal chemistry of botulinum, ricin and anthrax toxins. *Curr. Med. Chem.* **2005**, *12*, 667–690.

(5) Josko, D. Botulin toxin: a weapon in terrorism. *Clin. Lab. Sci.* **2004**, *17*, 30–34.

(6) Arnon, S. S.; Schechter, R.; Inglesby, T. V.; Henderson, D. A.; Bartlett, J. G.; Ascher, M. S.; Eitzen, E.; Fine, A. D.; Hauer, J.; Layton, M.; Lillibridge, S.; Osterholm, M. T.; O'Toole, T.; Parker, G.; Perl, T. M.; Russell, P. K.; Swerdlow, D. L.; Tonat, K. Botulinum toxin as a biological weapon: medical and public health management. *JAMA, J. Am. Med. Assoc.* **2001**, *285*, 1059–1070.

(7) Charles, P. D. Botulinum neurotoxin serotype A: a clinical update on non-cosmetic uses. *Am. J. Health-Syst. Pharm.* **2004**, *61*, S11–23.

(8) Foran, P. G.; Mohammed, N.; Lisk, G. O.; Nagwaney, S.; Lawrence, G. W.; Johnson, E.; Smith, L.; Aoki, K. R.; Dolly, J. O. Evaluation of the therapeutic usefulness of botulinum neurotoxin B, C1, E, and F compared with the long lasting type A. Basis for distinct durations of inhibition of exocytosis in central neurons. *J. Biol. Chem.* **2003**, *278*, 1363–1371.

(9) Simpson, L. L. Identification of the major steps in botulinum toxin action. *Annu. Rev. Pharmacol. Toxicol.* **2004**, *44*, 167–193.

(10) Amersdorfer, P.; Wong, C.; Smith, T.; Chen, S.; Deshpande, S.; Sheridan, R.; Marks, J. D. Genetic and immunological comparison of anti-botulinum type A antibodies from immune and non-immune human phage libraries. *Vaccine* **2002**, *20*, 1640–1648.

(11) Nowakowski, A.; Wang, C.; Powers, D. B.; Amersdorfer, P.; Smith, T. J.; Montgomery, V. A.; Sheridan, R.; Blake, R.; Smith, L. A.; Marks, J. D. Potent neutralization of botulinum neurotoxin by recombinant oligoclonal antibody. *Proc. Natl. Acad. Sci. U.S.A.* **2002**, *99*, 11346–11350.

(12) Willis, B.; Eubanks, L. M.; Dickerson, T. J.; Janda, K. D. The strange case of the botulinum neurotoxin: using chemistry and biology to modulate the most deadly poison. *Angew. Chem., Int. Ed.* **2008**, *47*, 8360–8379.

(13) Schmidt, J. J.; Stafford, R. G. A high-affinity competitive inhibitor of type A botulinum neurotoxin protease activity. *FEBS Lett.* **2002**, *532*, 423–426.

(14) Solaja, B. A.; Opsenica, D.; Smith, K. S.; Milhous, W. K.; Terzic, N.; Opsenica, I.; Burnett, J. C.; Nuss, J.; Gussio, R.; Bavari, S. Novel 4-aminoquinolines active against chloroquine-resistant and sensitive *P. falciparum* strains that also inhibit botulinum serotype A. *J. Med. Chem.* **2008**, *51*, 4388–4391.

(15) Boldt, G. E.; Eubanks, L. M.; Janda, K. D. Identification of a botulinum neurotoxin A protease inhibitor displaying efficacy in a cellular model. *Chem. Commun.* **2006**, 3063–3065.

(16) Boldt, G. E.; Kennedy, J. P.; Janda, K. D. Identification of a potent botulinum neurotoxin A protease inhibitor using in situ lead identification chemistry. *Org. Lett.* **2006**, *8*, 1729–1732.

(17) Moe, S. T.; Thompson, A. B.; Smith, G. M.; Fredenburg, R. A.; Stein, R. L.; Jacobson, A. R. Botulinum neurotoxin serotype A inhibitors: small molecule-mercaptoacetamide analogs. *Bioorg. Med. Chem.* **2009**, *17*, 3072–3079.

(18) Roxas-Duncan, V.; Enyedy, I.; Montgomery, V. A.; Eccard, V. S.; Carrington, M. A.; Lai, H.; Gul, N.; Yang, D. C. H.; Smith, L. A. Identification and biochemical characterization of small-molecule inhibitors of clostridium botulinum neurotoxin serptype A. *Antimicrob. Agents Chemother.* **2009**, *53*, 3478–3486.

(19) Lai, H.; Feng, M.; Roxas-Duncan, V.; Dakshanamurthy, S.; Smith, L. A.; Yang, D. C. H. Quinolinol and peptide inhibitors of zinc protease in botulinum neurotoxin A: effects of zinc ion and peptides on inhibition. *Arch. Biochem. Biophys.* **2009**, *491*, 75–84.

(20) Pang, Y.-P.; Vummenthala, A.; Mishra, R. K.; Park, J. G.; Wang, S.; Davis, J.; Millard, C. B.; Schmidt, J. J. Potent new small-molecule inhibitor of botulinum neurotoxin serotype A endopeptidase developed by synthesis-based computer-aided molecular design. *PLoS One* **2009**, *4*, No. e7730.

(21) Burnett, J. C.; Wang, C.; Nuss, J. E.; Nguyen, T. L.; Hermone, A. R.; Schmidt, J. J.; Gussio, R.; Wipf, P.; Bavari, S. Pharmacophore-guided lead optimization: the rational design of a non-zinc neurotoxin serotype a metalloprotease. *Bioorg. Med. Chem. Lett.* **2009**, *19*, 5811–5813.

(22) Burnett, J. C.; Ruthel, G.; Stegmann, C. M.; Panchal, R. G.; Nguyen, T. L.; Hermone, A. R.; Stafford, R. G.; Lane, D. J.; Kenny, T. A.; McGrath, C. F.; Wipf, P.; Stahl, A. M.; Schmidt, J. J.; Gussio, R.; Brunger, A. T.; Bavari, S. Inhibition of metalloprotease botulinum serotype A from a pseudo-peptide binding mode to a small molecule that is active in primary neurons. *J. Biol. Chem.* **2007**, *282*, 5004–5014.

(23) Burnett, J. C.; Opsenica, D.; Sriraghavan, K.; Panchal, R. G.; Ruthel, G.; Hermone, A. R.; Nguyen, T. L.; Kenny, T. A.; Lane, D. J.; McGrath, C. F.; Schmidt, J. J.; Vennerstrom, J. L.; Gussio, R.; Solaja, B. A.; Bavari, S. A refined pharmacophore identifies potent 4-amino-7-chloroquinoline-based inhibitors of the botulinum neurotoxin serotype A metalloprotease. *J. Med. Chem.* **2007**, *50*, 2127–2136.

(24) Capkova, K.; Hixon, M. S.; Pellett, S.; Barbieri, J. T.; Johnson, E. A.; Janda, K. D. Benzylidene cyclopentenediones: first irreversible inhibitors against botulinum neurotoxin A's zinc endopeptidase. *Bioorg. Med. Chem. Lett.* **2009**, *20*, 206–208.

(25) Wang, C.; Widom, J.; Petronijevic, F.; Burnett, J. C.; Nuss, J. E.; Bavari, S.; Gussio, R.; Wipf, P. Synthesis and biological evaluation of inhibitors of botulinum neurotoxin metalloprotease. *Heterocycles* **2009**, *79*, 487–520.

(26) Silvaggi, N. R.; Boldt, G. E.; Hixon, M. S.; Kennedy, J. P.; Tzipori, S.; Janda, K. D.; Allen, K. N. Structures of clostridium botulinum neurotoxin serotype A light chain complexed with small-molecule inhibitors highlight active-site flexibility. *Chem. Biol.* **2007**, *14*, 533–542.

(27) Silvaggi, N. R.; Wilson, D.; Tzipori, S.; Allen, K. N. Catalytic features of the botulinum neurotoxin A light chain revealed by high resolution structure of an inhibitory peptide complex. *Biochemistry* **2008**, *47*, 5736–5745.

(28) Schmidt, J. J.; Stafford, R. G. Fluorigenic substrates for the protease activities of botulinum neurotoxins, serotypes A, B, and F. *Appl. Environ. Microbiol.* **2003**, *69*, 297–303.

(29) Panchal, R. G.; Hermone, A. R.; Nguyen, T. L.; Wong, T. Y.; Schwarzenbacher, R.; Schmidt, J.; Lane, D.; McGrath, C.; Turk, B. E.; Burnett, J.; Aman, M. J.; Little, S.; Sausville, E. A.; Zaharevitz, D. W.; Cantley, L. C.; Liddington, R. C.; Gussio, R.; Bavari, S. Identification of small molecule inhibitors of anthrax lethal factor. *Nat. Struct. Mol. Biol.* **2004**, *11*, 67–72.

(30) Butler, M. M.; Cardinale, S. C.; Li, B.; Pai, R.; Ruthel, G.; Nuss, J. E.; Wanner, L. M.; Park, J.-B.; Rich, C.; Basu, A.; Mills, D.; Williams, J. D.; Peet, N. P.; Moir, D.; Bavari, S.; Bowlin, T. L. Unpublished results.

(31) Fu, Z.; Chen, S.; Baldwin, M. R.; Boldt, G. E.; Crawford, A.; Janda, K. D.; Barbieri, J. T.; Kim, J. J. Light chain of botulinum neurotoxin serotype A: structural resolution of a catalytic intermediate. *Biochemistry* **2006**, *45*, 8903–8911.

(32) Kumaran, D.; Rawat, R.; Ludivico, M. L.; Ahmed, S. A.; Swaminathan, S. Structure- and substrate-based inhibitor design for clostridium botulinum neurotoxin serotype A. *J. Biol. Chem.* **2008**, *283*, 18883–18891.